



Nuclear quantum effect on the elasticity of ice VII under pressure: A path-integral molecular dynamics study

Jun Tsuchiya ^{*}*Geodynamics Research Center, Ehime University, 2-5 Bunkyo-cho, Matsuyama, Ehime 790-8577, Japan*Motoyuki Shiga *Japan Atomic Energy Agency, 148-4 Kashiwanoha Campus, 178-4 Wakashiba, Kashiwa, Chiba 277-0871, Japan*

Shinji Tsuneyuki

*Department of Physics, The University of Tokyo Hongo, Bunkyo-ku, Tokyo 113-0033, Japan*Elizabeth C. Thompson *Department of Earth and Environmental Systems, The University of the South, 735 University Avenue, Sewanee, Tennessee 37383, USA*

(Received 5 July 2023; accepted 3 May 2024; published 20 June 2024)

We investigate the effect of nuclear quantum effects (NQE) of hydrogen atoms on the elasticity of ice VII at high pressure and ambient-temperature conditions using *ab initio* path-integral molecular dynamics (PIMD) calculations. We find that the NQEs of hydrogen contribute to the transition of ice VII from a static disordered structure to a dynamically disordered structure at pressures exceeding 40 GPa. This transition is characterized by a nonlinear increase in the elastic constants. A comparison of *ab initio* molecular dynamics, and PIMD calculations shows that NQEs increase the elastic constants of ice by about 20% at 70 GPa and 300 K.

DOI: [10.1103/PhysRevResearch.6.023302](https://doi.org/10.1103/PhysRevResearch.6.023302)

I. INTRODUCTION

Determining the structures and physicochemical properties of water ice (H_2O) is of fundamental importance to the fields of physics, chemistry, and planetary science. Although numerous experimental and theoretical studies have been performed on the 20 known crystalline polymorphs of water ice [1], their physical and chemical properties are not yet fully understood. An intrinsic challenge in the study of ices is that hydrogen is the lightest atom ($Z = 1$) and therefore hydrogen is extremely mobile, difficult to detect experimentally, and exhibits significant quantum effects.

The complexity and elusiveness of hydrogen is particularly evident when probing the behavior of ice at extreme pressures. As pressure is increased at ambient temperature, H_2O changes from ice VII to ice X (Figs. S1 and S2, Ref. [2]). Ice VII is a cubic crystal structure with static orientational disorder of the H_2O molecules while maintaining the ice rule [3]. This is possible because the oxygen atoms in ice VII are coordinated by four proton sites that are 50% occupied, and the orientation

of each H_2O molecule is dictated by which two of these four sites are occupied by hydrogen [4]. The ice VII structure and its physical properties are driven by this hydrogen bond network, which contains asymmetric hydrogen bonds [5]. In contrast, ice X is an ionic crystal with completely symmetric hydrogen bonds [6,7].

Broadly speaking, a transition in which the hydroxyl bonds (O-H) and hydrogen bonds ($\text{O}\cdots\text{H}$) in a crystal structure have the same length and form a straight line ($\text{O-H}\cdots\text{O} \approx 180^\circ$) at elevated pressures is called pressure-induced hydrogen bond symmetrization. This transition can be understood conceptually as the change in the behavior of hydrogen atoms as the potential surface between oxygen atoms changes from a double minima to a single minimum with increased pressure [8] (Fig. S1, [2]). In ice, hydrogen bond symmetrization can be described as a change in the state of hydrogen in the body-centered cubic sublattice of oxygen [9]. Previous studies have shown that in the ice VII to ice X transition, hydrogen changes from static (ice VII) to dynamically disordered (ice VII' and ice X') and then to symmetric hydrogen bonding states (ice X). In the dynamically disordered states of ice, hydrogen atoms move back and forth between two minima which exist between oxygen atoms due to thermal and quantum vibrational effects (i.e., tunneling effects) [10,11]. However, it is still challenging to directly observe such states of hydrogen under high pressure, and it has not been determined precisely at what pressures these phase transitions occur [12–16].

The existence of dynamically disordered ice has been established through *ab initio* molecular dynamics simulations

^{*}Also at Earth Life Science Institute (ELSI), Tokyo Institute of Technology, 2-12-1-1E-1 Ookayama, Meguro-ku, Tokyo 152-8550, Japan.

Published by the American Physical Society under the terms of the [Creative Commons Attribution 4.0 International license](https://creativecommons.org/licenses/by/4.0/). Further distribution of this work must maintain attribution to the author(s) and the published article's title, journal citation, and DOI.

(AIMD) [17], *ab initio* lattice dynamics calculations [15], and high-pressure x-ray diffraction studies of ice VII to X [14,16]. Since hydrogen atoms only weakly scatter x rays in x-ray diffraction experiments, changes in hydrogen bonding must be inferred by changes in the equation of state of ice under pressure [14,16]. These studies report that the transition to the dynamically disordered phases of ice VII (ice VII') and ice X (ice X') occur at 35–40 GPa and 50–60 GPa, respectively, and the transition to the ice X phase occurs at 90–110 GPa. However, these phase transition pressures are determined based on the small differences in curvature of the equations of state and thus have large errors and are still inconclusive.

Recently, the equation of state and vibrational properties of the high-pressure phases of ice have been reported using *ab initio* centroid molecular dynamics (CMD) calculations that can properly handle nuclear quantum effects (NQEs) [18]. The obtained equation of state shows a slight decrease in volume in the range of 20–60 GPa when compared to the equation of state obtained by conventional AIMD calculations, which treat nuclei as classical particles. However, it seems very difficult to infer the pressure at which hydrogen changes to a dynamically disordered state from such a small decrease in volume.

If this change of the state of hydrogen in ice VII to a dynamically disordered state under high pressure affects the equation of state, then it is expected that changes in elastic properties will appear more prominently. The sound velocities of high-pressure ice VII have been investigated by Brillouin scattering using polycrystalline and single-crystal samples at room-temperature conditions [19,20]. However, the former study reported that the elastic constants of ice increase monotonically and without discontinuities with increased pressure up to 100 GPa [19]. The latter study reported similar conclusions for measurements up to 103 GPa, but the elastic constants themselves were smaller than those measured for the polycrystalline samples of the earlier study [20]. On the other hand, it has been claimed that the elastic constants of ice VII containing a small amount (0.9 mol %) of sodium chloride show a softening of the elasticity at a pressure range of 42–54 GPa, corresponding to the dynamic disordered state of hydrogen [21].

In light of the reported lack of signs of a dynamically disordering state of hydrogen in the experimental elastic property of pure ice VII, this study investigated the temperature and quantum effects on it theoretically. As previously described, earlier CMD calculations have shown that NQEs affect the curvature of the equation of state in dynamically disordered states and that the elastic properties are expected to be affected accordingly. Therefore, in this study we performed first-principles path-integral molecular dynamics (PIMD) calculations [22–25] to determine the elastic properties of ice VII at room temperature and high pressures, taking into account NQEs, and compared them with AIMD calculations performed at the same (P - T) conditions.

II. METHODS

In this study, *ab initio* PIMD simulations based on the Born-Oppenheimer approximation were performed using the

PIMD software package [25] along with the open-source electronic structure calculation package QUANTUM ESPRESSO [26], which is based on density functional theory [27,28]. In order to properly evaluate the quantum effects of hydrogen nuclei in the high-pressure ice phases, the equation of state and elastic constants were calculated using PIMD at 300 K and high pressures, replicating the pressure-temperature conditions of most experiments on these phases. The generalized gradient approximation in the Perdew-Burke-Ernzerhof form (GGA-PBE) was used for the exchange-correlation functionals. There have been several attempts to incorporate van der Waals interaction to correctly calculate the ice structures, but the results are currently not strikingly good so far (e.g., [29–31]). Thus, there is no consensus situation on the functionals that should be used for the calculations of ice phases. Therefore, we focused our study on the extent to which different methods actually affect the equation of state and the elastic constants using GGA-PBE, as there have been many calculations of the high-pressure phases of ice using GGA-PBE, and it is useful to compare them. The norm-conserving pseudopotentials were used for the ionic inner-shell potentials of hydrogen and oxygen atoms [32]. The kinetic energy cutoff in the plane-wave expansion of the wave functions was set to 80 Ry. These pseudopotentials have been extensively tested in calculations of several hydrous minerals and ice [e.g., 5,33]. The sampling of the Brillouin zone was limited to the Γ point. The calculation of ice VII was modeled using a supercell ($3 \times 3 \times 3$ unit cells) containing 54 H_2O molecules. We performed calculations treating each of 162 atoms as the 10 and 32 beads in the simulation cells. Our PIMD simulations were within a canonical (NVT) ensemble where the number of atoms (N) and the cell volume (V) were set to a constant temperature (T), which was controlled by the massive Nosé-Hoover chains method. The time step Δt was set to 0.25 fs, and after equilibrating the system for about 1 ps, the trajectories were collected at least for 1 ps to accumulate statistics. To enable comparison with PIMD, AIMD calculations were also performed on the same system and under the same calculation conditions, except for the number of beads.

In this study it was important to estimate the effect of NQEs on pressure and stress. Because of the spatial extent of the hydrogen nuclei, the quantum effects of the nuclei on the pressure are also expected to be significant. To properly incorporate this effect, a virial correction was performed, which adds the product of the distance from the centroid of the beads and the force applied to each bead [34].

The isothermal elastic constants C_{ij} s were calculated from the linear relationship of stress-strain by applying a strain of ± 0.01 and time-averaging the induced stresses. We confirmed that a linear relation was ensured for this strain range using a previously established methodology [5].

III. RESULTS

First, we compare the volumes of ice VII under pressure at 300 K calculated using PIMD and AIMD (Fig. 1). We also plotted the volumes of hydrogen-ordered ice VIII and X at static 0 K under pressure [5]. The volumes obtained

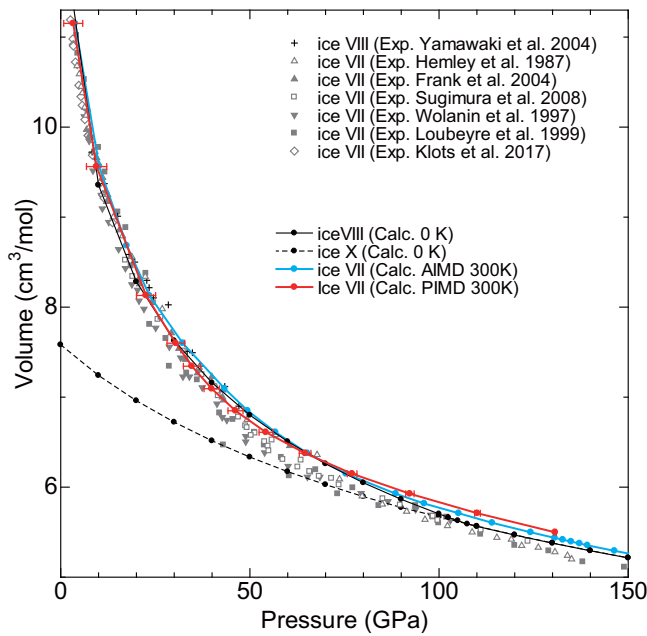


FIG. 1. The pressure-volume (P - V) relationship of ice VII. The black solid and dashed lines indicate the P - V curves of ice VIII (asymmetric hydrogen bond with ordered hydrogen positions) and ice X (symmetric hydrogen bonds) at static 0-K condition, respectively. The volumes of the ice X phase in the metastable state (0–110 GPa) have been calculated under the condition that the original space group ($Pm\bar{3}m$) is maintained. The red and blue lines indicate the P - V relationships of ice VII at 300 K obtained by PIMD and AIMD simulations, respectively. The volumes determined by PIMD simulation are smaller than those obtained by AIMD simulation at 20–70 GPa. The gray symbols indicate the volume of ice VII phase reported so far by high-pressure x-ray diffraction experiments [9,14,35–39]. The experimental data of Sugimura *et al.* [14] and Hemley *et al.* [9] were reanalyzed using the recent pressure scales of Dorogokupets and Dewaele [40] and Dewaele *et al.* [41], respectively.

with PIMD are very slightly smaller than those obtained with AIMD between 20 and 70 GPa. The calculated P - V relationships, including the static 0-K results, are generally larger than the experimental values [9,35,37–39] for all pressure conditions, and this difference is likely largely due to the exchange-correlation functional, GGA-PBE, used in this study [29]. At the high-pressure conditions above 70 GPa, the volume obtained by PIMD is larger than that of AIMD due to quantum fluctuations of the hydrogen nuclei. These results are consistent with the equation of state of ice VII obtained for CMD [18]. A comparison of theoretical calculations of the P - V relationships at static 0 K and 300 K shows that the difference between the ordered and dynamically disordered states of hydrogen is very small, making it difficult to discuss the hydrogen state using only the equation of state.

To investigate the influence of NQEs on the hydrogen-bonding properties of ice VII under pressure, the radial distribution function (RDF) of ice VII was obtained using both PIMD and AIMD results, as shown in Fig. 2. The RDF obtained by PIMD exhibits a higher distribution between the covalent ($R_{O-H} \sim 1 \text{ \AA}$) and hydrogen bond distances ($R_{O\cdots H} \sim 1.3\text{--}1.6 \text{ \AA}$) at lower pressures than that obtained by AIMD. This suggests that the NQEs enhance the appearance of the dynamically disordered state of hydrogen and associated partially symmetric hydrogen bond state at lower pressures.

Next, the effects of the disordering of hydrogen in the high-pressure phases of ice on the elastic constants were investigated (Table I, Fig. 3). Figure 3 shows the elastic constants of ice VII/VIII and ice X under pressure. The solid and dashed black lines are the elastic constants of ice VIII and X previously reported at static 0-K conditions [5]. The elastic constants of ice VIII (solid black lines), which has ordered hydrogen positions, increases steeply at 100–110 GPa due to the symmetrization of the hydrogen bonds. The elastic

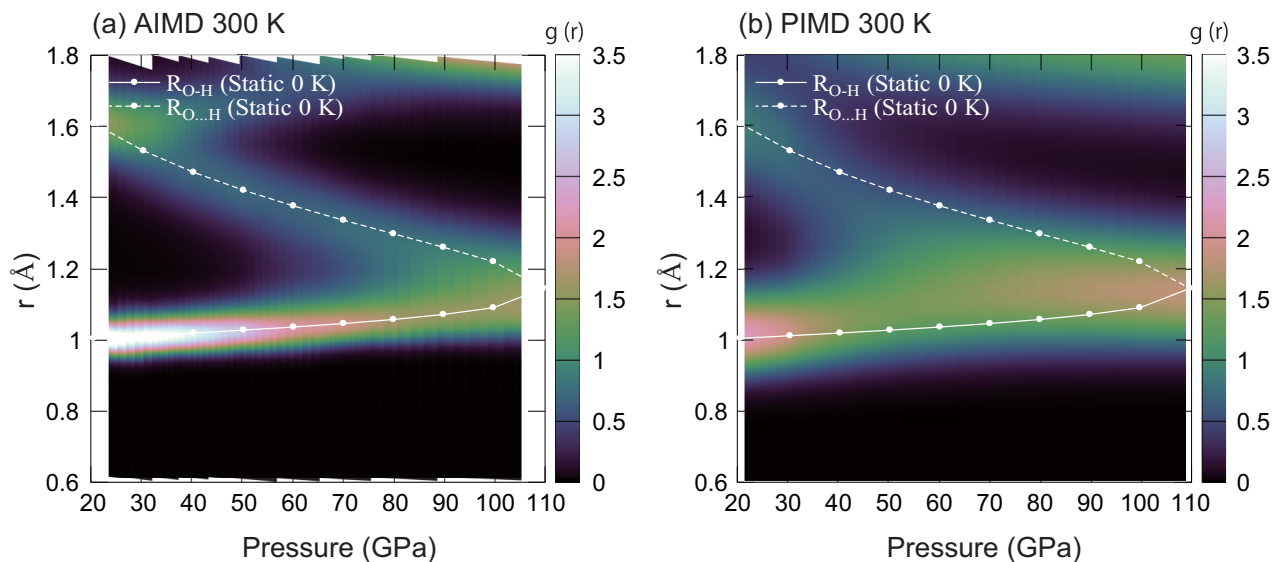


FIG. 2. The radial distribution function (RDF) under pressure. The white solid and dashed lines are the OH and $O\cdots H$ distances for the ice VIII phase, respectively, at static 0-K conditions by structural optimization that does not take into account the quantum effects of nuclei.

TABLE I. The high-pressure elastic constants, and the bulk (B) and shear (G) moduli (Hill average) of ice VII at 300 K calculated by the PIMD method ($N_{\text{beads}} = 32$).

P (GPa)	V (cm ³ /mol)	C_{11}	C_{12}	C_{44}	B	G
30.4	7.600	179.84	98.13	114.62	125.37	75.83
34.7	7.343	189.83	107.63	133.94	135.03	83.58
39.9	7.093	223.05	123.73	144.97	156.84	94.43
46.2	6.849	260.68	153.85	181.22	189.46	111.35
54.2	6.610	334.55	214.32	219.19	254.40	131.03
64.6	6.377	399.59	272.04	250.22	314.56	145.49
77.0	6.150	472.06	341.31	291.47	385.15	161.64
130.7	5.498	670.62	535.50	379.87	580.54	194.14

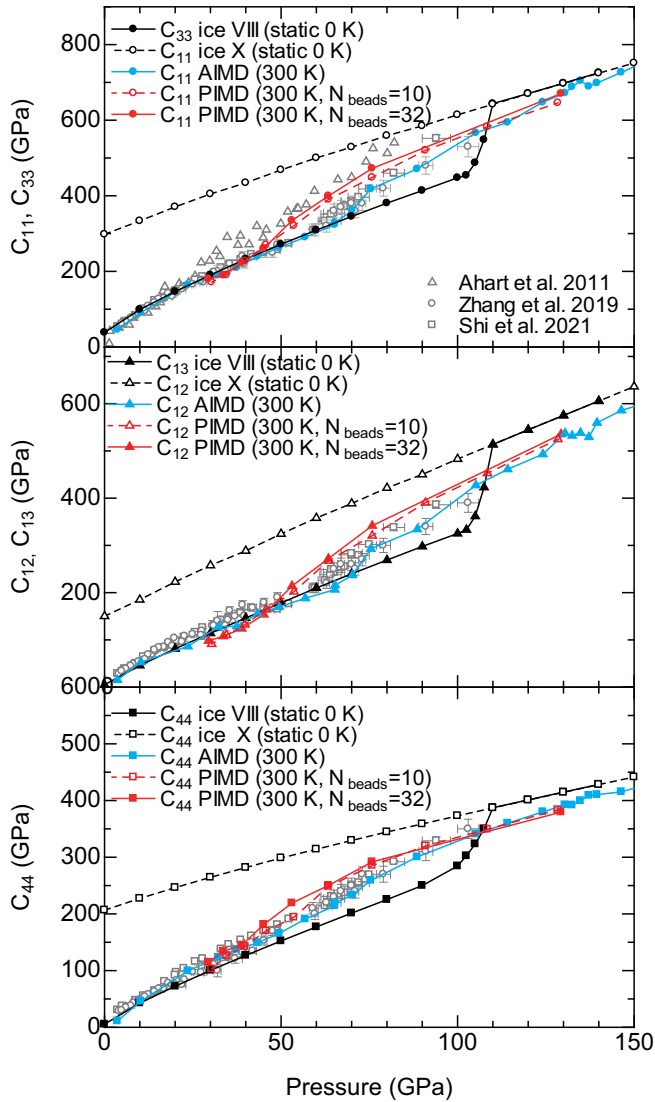


FIG. 3. The elastic constants of ice VII/VIII and ice X under pressure. The black solid and dashed lines indicate the elastic constants of ice VIII and X at static 0-K conditions, respectively [5]. The elastic constants of the ice X phase in the metastable state (0–110 GPa) have been calculated under the condition that the original space group ($Pm\bar{3}m$) is maintained. The red and blue lines indicate the C_{ij} of ice VII at 300 K determined by PIMD ($N_{\text{beads}} = 32$) and AIMD simulations, respectively. Dashed red lines indicate PIMD simulation with smaller number of beads ($N_{\text{beads}} = 10$). The open symbols are previous Brillouin scattering measurements [19–21].

constants of metastable ice X with symmetric hydrogen bonds (dashed black lines) below ~ 110 GPa are significantly larger than those of ice VIII. The main difference between these structures is whether the hydrogen bonds are symmetrized or not. Thus, even partial hydrogen bond symmetrization at finite-temperature conditions in ice VII, as indicated in RDF (Fig. 2), is expected to contribute to an increase in the elastic constants.

Then we compared the elastic constants of the ordered (ice VIII) and static disordered states of hydrogen. The pressure dependence of the elastic constants of the disordered states of hydrogen were calculated at static 0 K (Fig. S3, [2]). The results show that the elastic constants of those structures are almost the same as those of the ice VIII. From these results, we confirm that the disordered structures themselves do not contribute to the increase in the elastic constants.

Finally, we compare the elastic constants obtained by AIMD, PIMD, and Brillouin scattering experiments [19,20]. All of AIMD, PIMD, and experimental values show almost parallel changes to the static 0-K elastic constants at low-pressure conditions, which may be explained only by differences in temperature conditions in the static disordered ice VII phase. However, as pressure is increased, the PIMD, the experimental [20], and the AIMD results begin to notably deviate from the static 0-K values at 40, 60, and 70 GPa, respectively. These increases of the elastic constants are likely caused by the dynamic behavior of hydrogen atoms. The comparison of AIMD and PIMD results indicates that NQE contributes significantly to the increase in elastic constants above 40 GPa and by as much as 20% at around 70 GPa at 300-K condition. Comparing the pressure change in the elastic constants at static 0 K with the experimental elastic constants [20,21], the change is not smooth or softening but rather, hardening. The pressure at which this nonlinear increase in elastic constants occurs is different between the Brillouin scattering experiment and PIMD results. Possible reasons for this discrepancy could be due to the approximation of the exchange-correlation functional in the calculations or because the Brillouin scattering peak is hidden by the diamond peak at about 50 GPa, making it difficult to measure.

IV. CONCLUSIONS

We investigated the effects of the nuclear quantum effects (NQEs) on the elastic constants of high-pressure ice phases. We show that the elastic constants of ice increase nonlinearly

due to the partial hydrogen bond symmetrization associated with the change of the state of hydrogen in ice phase VII to a dynamically disordered state under pressure. The transition from a static to a dynamically disordered phase occurs at about 40 GPa. The NQEs affect the elastic constants in the pressure range of 40–100 GPa at 300 K and are most pronounced at around 70 GPa. NQEs contribute to the increase in elastic constants by up to 20% at room temperature and high pressure. This finding implies that the experimentally elusive structural feature of dynamically disordered states, which is promoted by the tunneling effect of hydrogen nuclei in the ice phase, affects macroscopic properties such as elastic constants at ambient temperature.

ACKNOWLEDGMENTS

This work was supported by Japan Society for the Promotion of Science KAKENHI Grant Nos. JP20K04043, JP20K04126, JP23K04670, and JP23H01273. The computation was carried out using the General Projects on supercomputer “Flow” at the Information Technology Center, Nagoya University, and the facilities of the Supercomputer Center, Institute for Solid State Physics, University of Tokyo. M.S. was supported a “Hydrogenomics” grant through Grants-in-Aid for Scientific Research on Innovative Areas, MEXT, Japan, JSPS KAKENHI (JP18H05519, JP21H01603), and the JAEA Supercomputer Project.

-
- [1] T. C. Hansen, The everlasting hunt for new ice phases, *Nat. Commun.* **12**, 3161 (2021).
- [2] See Supplemental Material at <http://link.aps.org/supplemental/10.1103/PhysRevResearch.6.023302> for the structure and phase diagram of the high pressure ice phases.
- [3] J. D. Bernal and R. H. Fowler, A theory of water and ionic solution, with particular reference to hydrogen and hydroxyl ions, *J. Chem. Phys.* **1**, 515 (1933).
- [4] M. Guthrie, R. Boehler, J. J. Molaison, B. Habler, A. M. dos Santos, and C. Tulk, Structure and disorder in ice VII on the approach to hydrogen-bond symmetrization, *Phys. Rev. B* **99**, 184112 (2019).
- [5] J. Tsuchiya and T. Tsuchiya, First principles calculation of the elasticity of ice VIII and X, *J. Chem. Phys.* **146**, 014501 (2017).
- [6] W. B. Holzapfel, On the symmetry of the hydrogen bonds in ice VII, *J. Chem. Phys.* **56**, 712 (1972).
- [7] K. S. Schweizer and F. H. Stillinger, High pressure phase transitions and hydrogen-bond symmetry in ice polymorphs, *J. Chem. Phys.* **80**, 1230 (1984).
- [8] J. Tsuchiya and E. C. Thompson, The role of hydrogen bonds in hydrous minerals stable at lower mantle pressure conditions, *Prog. Earth Planet. Sci.* **9**, 63 (2022).
- [9] R. J. Hemley, A. P. Jephcoat, H. K. Mao, C. S. Zha, L. W. Finger, and D. E. Cox, Static compression of H₂O-ice to 128 GPa (1.28 Mbar), *Nature (London)* **330**, 737 (1987).
- [10] M. Benoit, D. Marx, and M. Parrinello, Tunnelling and zero-point motion in high-pressure ice, *Nature (London)* **392**, 258 (1998).
- [11] J. A. Morrone, L. Lin, and R. Car, Tunneling and delocalization effects in hydrogen bonded systems: A study in position and momentum space, *J. Chem. Phys.* **130**, 204511 (2009).
- [12] K. Aoki, H. Yamawaki, M. Sakashita, and H. Fujihisa, Infrared absorption study of the hydrogen-bond symmetrization in ice to 110 GPa, *Phys. Rev. B* **54**, 15673 (1996).
- [13] A. F. Goncharov, V. V. Struzhkin, M. S. Somayazulu, R. J. Hemley, and H. K. Mao, Compression of ice to 210 GPa: Infrared evidence for a symmetric hydrogen-bonded phase, *Science* **273**, 218 (1996).
- [14] E. Sugimura, T. Iitaka, K. Hirose, K. Kawamura, N. Sata, and Y. Ohishi, Compression of H₂O ice to 126 GPa and implications for hydrogen-bond symmetrization: Synchrotron x-ray diffraction measurements and density-functional calculations, *Phys. Rev. B* **77**, 214103 (2008).
- [15] R. Caracas, Dynamical instabilities of ice X, *Phys. Rev. Lett.* **101**, 085502 (2008).
- [16] A. S. J. Méndez, F. Trybel, R. J. Husband, G. Steinle-Neumann, H. P. Liermann, and H. Marquardt, Bulk modulus of H₂O across the ice VII-ice X transition measured by time-resolved x-ray diffraction in dynamic diamond anvil cell experiments, *Phys. Rev. B* **103**, 064104 (2021).
- [17] M. Benoit, A. H. Romero, and D. Marx, Reassigning hydrogen-bond centering in dense ice, *Phys. Rev. Lett.* **89**, 145501 (2002).
- [18] T. Ikeda, First principles centroid molecular dynamics simulation of high pressure ices, *J. Chem. Phys.* **148**, 102332 (2018).
- [19] M. Ahart, M. Somayazulu, S. A. Gramsch, R. Boehler, H. K. Mao, and R. J. Hemley, Brillouin scattering of H₂O ice to megabar pressures, *J. Chem. Phys.* **134**, 124517 (2011).
- [20] J. S. Zhang, M. Hao, Z. Ren, and B. Chen, The extreme acoustic anisotropy and fast sound velocities of cubic high-pressure ice polymorphs at Mbar pressure, *Appl. Phys. Lett.* **114**, 191903 (2019).
- [21] W. Shi, N. Sun, X. Li, Z. Mao, J. Liu, and V. B. Prakapenka, Single-crystal elasticity of high-pressure ice up to 98 GPa by Brillouin scattering, *Geophys. Res. Lett.* **48**, e2021GL092514 (2021).
- [22] D. Marx and M. Parrinello, *Ab initio* path-integral molecular dynamics, *Z. Phys. B* **95**, 143 (1994).
- [23] D. Marx and M. Parrinello, *Ab initio* path integral molecular dynamics: Basic ideas, *J. Chem. Phys.* **104**, 4077 (1996).
- [24] M. E. Tuckerman, D. Marx, M. L. Klein, and M. Parrinello, Efficient and general algorithms for path integral Car-Parrinello molecular dynamics, *J. Chem. Phys.* **104**, 5579 (1996).
- [25] M. Shiga, M. Tachikawa, and S. Miura, A unified scheme for *ab initio* molecular orbital theory and path integral molecular dynamics, *J. Chem. Phys.* **115**, 9149 (2001).
- [26] P. Giannozzi, S. Baroni, N. Bonini, M. Calandra, R. Car, C. Cavazzoni, D. Ceresoli, G. L. Chiarotti, M. Cococcioni, I. Dabo, A. Dal Corso, S. de Gironcoli, S. Fabris, G. Fratesi, R. Gebauer, U. Gerstmann, C. Gougoussis, A. Kokalj, M. Lazzeri, L. Martin-Samos *et al.*, QUANTUM ESPRESSO: A modular and open-source software project for quantum simulations of materials, *J. Phys.: Condens. Matter* **21**, 395502 (2009).
- [27] P. Hohenberg and W. Kohn, Inhomogeneous electron gas, *Phys. Rev.* **136**, B864 (1964).

- [28] W. Kohn and L. J. Sham, Self-consistent equations including exchange and correlation effects, *Phys. Rev.* **140**, A1133 (1965).
- [29] B. Santra, J. Klimes, D. Alfe, A. Tkatchenko, B. Slater, A. Michaelides, R. Car, and M. Scheffler, Hydrogen bonds and van der Waals forces in ice at ambient and high pressures, *Phys. Rev. Lett.* **107**, 185701 (2011).
- [30] B. Santra, J. Klimes, A. Tkatchenko, D. Alfe, B. Slater, A. Michaelides, R. Car, and M. Scheffler, On the accuracy of van der Waals inclusive density-functional theory exchange-correlation functionals for ice at ambient and high pressures, *J. Chem. Phys.* **139**, 154702 (2013).
- [31] J. G. Brandenburg, T. Maas, and S. Grimme, Benchmarking DFT and semiempirical methods on structures and lattice energies for ten ice polymorphs, *J. Chem. Phys.* **142**, 124104 (2015).
- [32] N. Troullier and J. L. Martins, Efficient pseudopotentials for plane-wave calculations, *Phys. Rev. B* **43**, 1993 (1991).
- [33] J. Tsuchiya and T. Tsuchiya, Elastic properties of δ -AlOOH under pressure: First principles investigation, *Phys. Earth Planet. Inter.* **174**, 122 (2009).
- [34] G. J. Martyna, A. Hughes, and M. E. Tuckerman, Molecular dynamics algorithms for path integrals at constant pressure, *J. Chem. Phys.* **110**, 3275 (1999).
- [35] H. Yamawaki, H. Fujihisa, M. Sakashita, A. Nakayama, and K. Aoki, Powder X-ray diffraction study of the volume change of ice VIII under high pressure, *Physica B* **344**, 260 (2004).
- [36] M. R. Frank, Y. Fei, and J. Hu, Constraining the equation of state of fluid H₂O to 80 GPa using the melting curve, bulk modulus, and thermal expansivity of ice VII, *Geochim. Cosmochim. Acta* **68**, 2781 (2004).
- [37] E. Wolanin, P. Pruzan, J. C. Chervin, B. Canny, M. Gauthier, D. Häusermann, and M. Hanfland, Equation of state of ice VII up to 106 GPa, *Phys. Rev. B* **56**, 5781 (1997).
- [38] P. Loubeyre, R. LeToullec, E. Wolanin, M. Hanfland, and D. Häusermann, Modulated phases and proton centring in ice observed by X-ray diffraction up to 170 GPa, *Nature (London)* **397**, 503 (1999).
- [39] S. Klotz, K. Komatsu, H. Kagi, K. Kunc, A. Sano-Furukawa, S. Machida, and T. Hattori, Bulk moduli and equations of state of ice VII and ice VIII, *Phys. Rev. B* **95**, 174111 (2017).
- [40] P. I. Dorogokupets and A. Dewaele, Equations of state of MgO, Au, Pt, NaCl-B1, and NaCl-B2: Internally consistent high-temperature pressure scales, *High Pressure Res.* **27**, 431 (2007).
- [41] A. Dewaele, P. Loubeyre, and M. Mezouar, Equations of state of six metals above 94 GPa, *Phys. Rev. B* **70**, 094112 (2004).